

Solid-state ^{13}C n.m.r. study on miscibility of polyoxymethylene/terpenephenol blends

Yuichiro Egawa*, Shinichiro Imanishi and Akiko Matsumoto

Research Center, Daicel Chemical Industries, Ltd, Himeji, Hyogo 671-12, Japan

and Fumitaka Horii*

Institute for Chemical Research, Kyoto University, Uji, Kyoto 611, Japan

(Received 13 February 1996; revised 12 March 1996)

The mixing state in polyoxymethylene (POM) and terpenephenol (TPh) blends prepared by melt-blending has been studied by transmission electron microscopy (TEM), Fourier-transform infrared (FTi.r.) spectroscopy and high-resolution solid-state ^{13}C n.m.r. spectroscopy. On the basis of these morphological and spectral measurements, the following facts have been revealed: (i) POM/TPh (5/5) blend is homogeneous on a scale of a μm ; (ii) the intermolecular hydrogen-bonding interaction between POM and TPh makes their blends miscible; (iii) a level of this interaction exhibits a significant compositional dependence; (iv) the noncrystalline phase of POM is preferentially miscible with TPh, while a part of POM is still crystallizable; and (v) the size of the phase-separated domain for POM/TPh (5/5) blend is estimated to be *ca.* 1 nm in the noncrystalline phase by the ^1H spin diffusion analysis, suggesting the almost homogeneous mixing on a molecular level. Copyright © 1996 Elsevier Science Ltd.

(Keywords: polyoxymethylene; terpenephenol; CP/MAS ^{13}C n.m.r.)

INTRODUCTION

Polyoxymethylene (POM), which is a highly crystalline polymer, exhibits high mechanical strength and excellent resistivity against heat and solvents. From these characteristic properties, it is one of the commercially important materials in the field of engineering plastics. In spite of its potentially wide availability, POM has not been frequently applied to polymer blends due to its poor solubility in various solvents. Of the miscible polymers with POM, only novolak resin¹ and polyvinylphenol (PVPh)^{2,3} have been reported at present. From a viewpoint of developing polymer blends with new function, a research of polymer blends including POM seems to be of great interest.

French *et al.* reported that intermolecular hydrogen-bonding interaction between POM and other polymers is a driving force for miscible blends³. So, this suggests that polymers possessing phenolic OH groups could form the strong intermolecular hydrogen-bonding with POM. As a potentially miscible polymer with POM, we focus our attention on terpenephenol (TPh) which is composed of terpene and phenolic moieties as shown in *Figure 1*.

The major object of this paper is to characterize the miscibility of POM/TPh blends. We apply transmission electron microscopy (TEM), Fourier-transform infrared (FTi.r.) spectroscopy and high-resolution solid-state n.m.r. spectroscopy as tools for the evaluation of miscibility. In order to discriminate between the contributions from noncrystalline and crystalline phases in the blends, selective observations of these phases are

performed by using ^{13}C spin-echo and CPT1⁴ pulse sequences. The level of miscibility for POM/TPh blends is also estimated by the spin-diffusion experiment, including the Goldman–Shen pulse sequence⁵.

EXPERIMENTAL

Materials

Polyoxymethylene (POM, Duracon M90-44) was supplied by Polyplastics Co., Inc. Terpenephenol (TPh, Mighty Ace K-125) was purchased from Yasuhara Chemical Co., Inc., a number-average molecular weight being *ca.* 600. An aliphatic and aromatic proton ratio of TPh was determined to be 91:9 by ^1H n.m.r. spectroscopy. An X-ray diffraction analysis revealed TPh to be a noncrystalline polymer. Both materials were used without further purification.

Preparation of samples

Component ratios of POM/TPh blends range from 5/5 to 9/1 (w/w). These blends were prepared by means of melt-blending using Haake Brabender PL-3000 with a screw rotation speed of 50 rpm at 190°C for 5 min, followed by a compression moulding into plaques of 2 mm thickness at 200°C.

Measurements

Transmission electron microscopic (TEM) observations were performed on a HITACHI H-600 electron microscope at an accelerating voltage of 100 kV. Ultra-thin film slices (*ca.* 0.1 μm thickness) of the blends were prepared using a microtomy technique for the

* To whom correspondence should be addressed

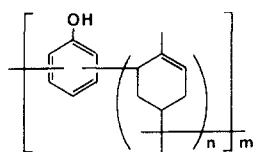


Figure 1 Structure of terphenol (TPh)

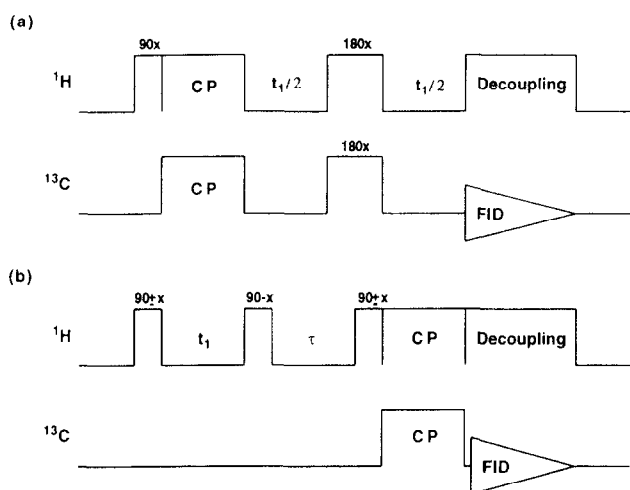


Figure 2 Pulse sequences employed in this work: (a) ^{13}C spin-echo pulse sequence; (b) pulse sequence combined with Goldman-Shen pulse sequence and CP technique

measurements. The staining with ruthenium tetroxide (RuO_4) vapour was performed according to the method described by Trent *et al.*⁶

Fourier-transform infrared (FTi.r.) spectra were recorded on a Perkin Elmer 1600 FTi.r. spectrometer at room temperature. Scans of more than 100 and a peak resolution of 2 cm^{-1} were employed. Since cast films of POM/TPh blends were unable to be prepared due to their poor solubility, extra-thin film slices ($1\text{--}2\ \mu\text{m}$ thickness) of the blends were prepared in a similar way to the samples used on TEM observations described above.

High-resolution solid-state n.m.r. measurements were carried out on a JEOL JNM-GX270WB spectrometer at a ^{13}C frequency of 67.9 MHz at room temperature. ^1H 90° pulse width of $4.5\ \mu\text{s}$ was employed, corresponding to a radio frequency field strength of 56 kHz. ^1H irradiation frequency was 3 ppm downfield from the resonance for tetramethylsilane (Me_4Si). Spectral width encompassed a range of 27 kHz and data points of 8 k were employed. ^{13}C chemical shifts were referenced externally to the CH resonance line of adamantane, 29.5 ppm from Me_4Si . Representative pulse sequences used in this work are shown in Figure 2.

CP/MAS ^{13}C spectra were measured at a contact time of 2 ms, pulse delay of 5 s and MAS rate of 4 kHz. ^{13}C spin-echo and CPT1⁴ pulse sequences were employed for selective observations of the noncrystalline and crystalline components in POM or POM/TPh blends, respectively. Fixed delay times t_1 for the relaxations were $40\ \mu\text{s}$ for the spin-echo pulse sequence and 3 s for the CPT1 pulse sequence. Other conditions for these two pulse sequences were the same as used for the CP/MAS measurements. On measurement of ^1H spin-lattice relaxation time ($T_{1\text{H}}$), ^1H spin-lattice relaxation time in the rotating frame ($T_{1\rho\text{H}}$) and ^1H spin-spin relaxation

time ($T_{2\text{H}}$), ^1H magnetizations were indirectly detected as ^{13}C signals, using a contact time of 0.1 ms and pulse delay of 5 s. ^{13}C - ^1H cross-polarization relaxation time (T_{CH}) values were obtained by varying a contact time. In the ^1H spin-diffusion experiment, a fixed delay time t_1 of $40\ \mu\text{s}$ was employed in the Goldman-Shen pulse sequence.

RESULTS AND DISCUSSION

TEM observations

A transmission electron microscopic (TEM) study was employed for morphological observation of POM and POM/TPh blends. TEM observations were carried out after staining with ruthenium tetroxide (RuO_4) vapour⁶. Figure 3a shows a TEM micrograph of POM. In Figure 3a, orientation of POM crystals is observed, and also radially oriented lamellar striations, which are parts of a spherulite, are formed in agreement with the previous finding⁷. In contrast, the POM/TPh (7/3) blend is phase-separated, as seen in Figure 3b, where dark particles with a diameter smaller than $2\ \mu\text{m}$ are dispersed in a rather homogeneous matrix. Since TPh is more readily stained under the condition employed here, the dispersed particles should be the region composed of TPh. However, the apparent fraction of the TPh particles seems to be greatly lower compared to the real weight fraction (0.3) of TPh in this blend. Accordingly most of TPh may be included in the matrix, resulting in the morphology of the matrix evidently different from that for POM. Figure 3c shows a TEM micrograph of a POM/TPh (5/5) blend. Only a finely mixed matrix phase is observed without such dispersed particles for the POM/TPh (7/3) blend, indicating that the POM/TPh (5/5) blend is homogeneous on a scale of a μm .

FTi.r. experiments

Intermolecular interaction is considered to play a key role in the miscibility of polymer blends⁸. We have examined the intermolecular hydrogen-bonding between POM and TPh by Fourier-transform infrared (FTi.r.) spectroscopy. Figure 4 shows the i.r. absorption spectra in the OH stretching vibration region ($3800\text{--}3000\text{ cm}^{-1}$) for POM, TPh and the POM/TPh blends, which are recorded on the absorbance scale. In TPh (Figure 4e), the absorption band for the free OH group appears at 3600 cm^{-1} , which is in good agreement with the previous result for phenol². Moreover, two ambiguous broad absorptions are observed in the associated OH stretching region of $3520\text{--}3420\text{ cm}^{-1}$. The OH band at 3520 cm^{-1} may be assigned to the self-associated OH group undergoing the dimeric interaction of TPh, on the analogy of the case for the POM/novolac resin blend¹. Another OH band at 3420 cm^{-1} may be ascribed to a different type of self-associated OH group possibly participating in the polymeric interaction of TPh, though there is no evidence for this assignment. When TPh is mixed with POM, these absorptions of TPh are somewhat changed in line shape as shown in Figures 4a-d; a different absorption band with almost mono-peak appears around 3428 cm^{-1} concomitantly with disappearance of two bands at 3600 and 3520 cm^{-1} . Such i.r. spectral change suggests that most of OH groups of TPh are associated with the intermolecular hydrogen-bonding with POM in the blend in accordance with the previous cases^{2,8}.

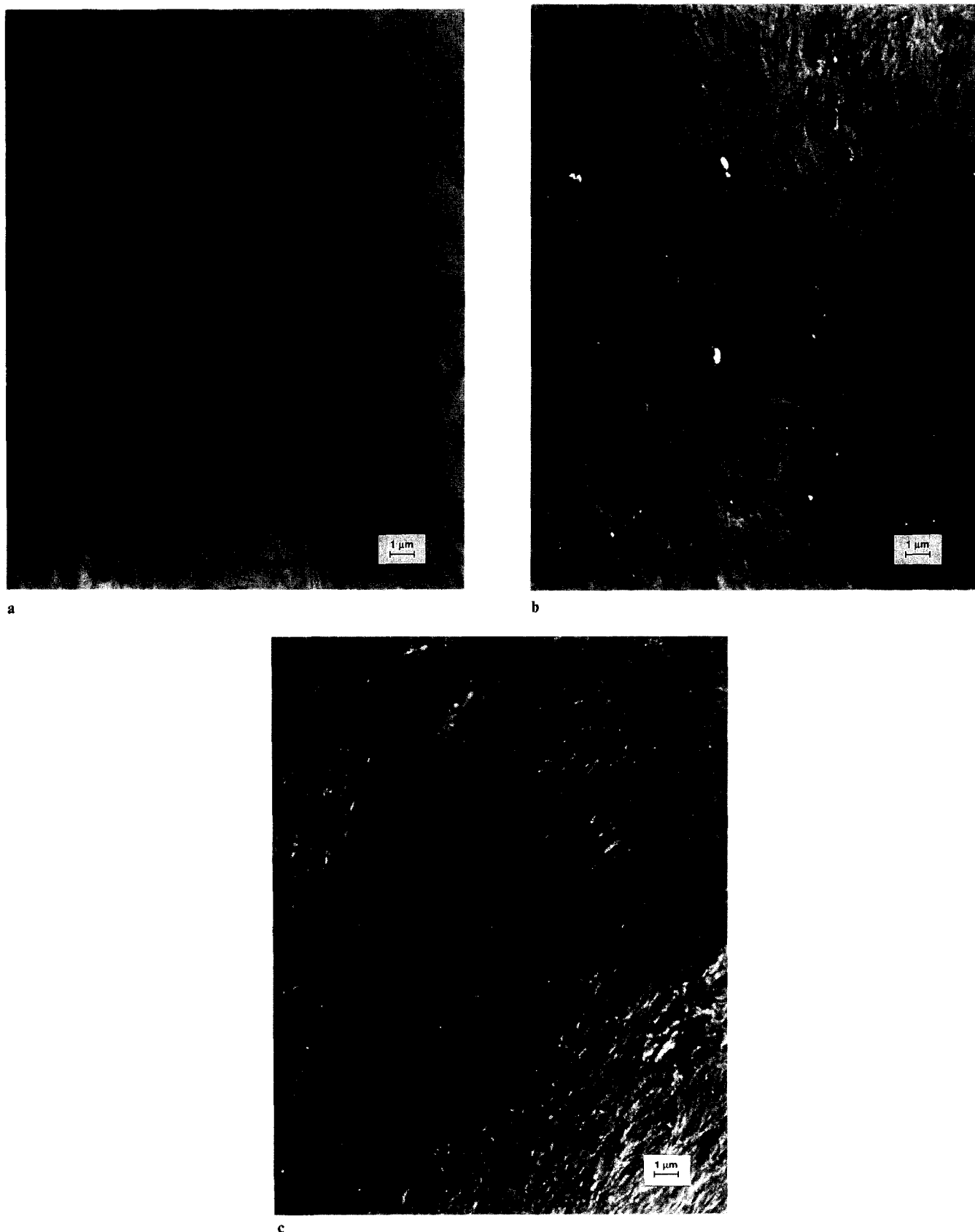


Figure 3 Electron micrographs for different samples stained with RuO_4 vapour: (a) POM; (b) POM/TPh = 7/3; (c) POM/TPh = 5/5

On the other hand, POM shows the characteristic i.r. absorptions in the region of $1200\text{--}900\text{ cm}^{-1}$ (Figure 5). Two complex i.r. bands appear around $1000\text{--}900$ and $1150\text{--}1070\text{ cm}^{-1}$, which are assigned to the methylene rocking and skeletal stretching vibration, and C–O

stretching vibration, respectively⁹. These bands are changed in shape with increasing TPh content in the blends. Especially, the bands at 990 cm^{-1} and 1130 cm^{-1} evidently increase in intensity as the content of TPh increases. Similar spectral changes around 990 cm^{-1} and

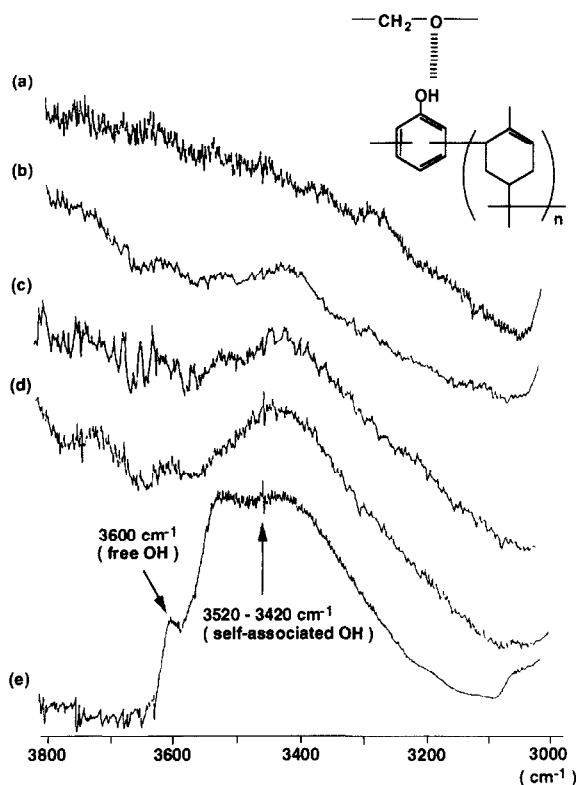


Figure 4 FTIR spectra for different samples in the OH stretching vibration region ($3800\text{--}3000\text{ cm}^{-1}$): (a) POM; (b) POM/TPh = 9/1; (c) POM/TPh = 7/3; (d) POM/TPh = 5/5; (e) TPh

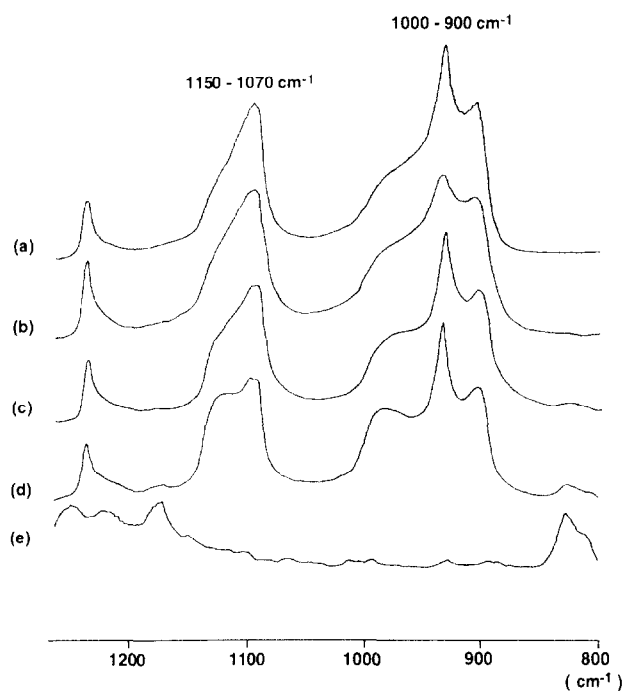


Figure 5 FTIR spectra for different samples in ether stretching vibration region ($1250\text{--}800\text{ cm}^{-1}$): (a) POM; (b) POM/TPh = 9/1; (c) POM/TPh = 7/3; (d) POM/TPh = 5/5; (e) TPh

1130 cm^{-1} have been observed for some POM specimens and various explanations for such spectral regions have been proposed¹⁰⁻¹². For example, those absorption bands have been assigned to the planar zig-zag conformations in the noncrystalline region¹⁰, to the conformational defects in helical chains¹¹, or to the folded-chain

(needle-like) crystals¹², though no clear conclusion for those spectral changes has yet been obtained. In any event, based on the i.r. spectroscopic change depending on the content of TPh, it was assumed that the intermolecular interaction between the ether oxygen of POM and the OH group of TPh induces the structural change of POM.

High-resolution solid-state n.m.r. spectroscopy

Figure 6 shows CP/MAS ^{13}C spectra for POM, TPh and their blends obtained at room temperature. The phenolic carbon signal of TPh is observed at 153.2 ppm in Figure 6e and significantly shifts downfield with increasing content of POM; for example, the corresponding line appears at 154.8 ppm for the POM/TPh (9/1) blend as shown in Figure 6b. This means that the electron density around the phenolic carbon will decrease probably as a result of the intermolecular interaction between the phenolic OH group and the ether oxygen atom.

In contrast to the phenolic carbon of TPh, the methylene carbon of POM seems to exhibit no clear change in line shape or chemical shift as shown in Figure 6. However, since the mixing will be induced in different ways in the crystalline and noncrystalline phases¹³, we have done selective ^{13}C n.m.r. observations of the respective phases by using ^{13}C spin-echo and CPT1 pulse sequences. In Figure 7 the spin-echo spectra for POM, TPh and their blends are displayed, where the noncrystalline phase of POM is emphasized due to its longer ^{13}C spin-spin relaxation time (T_{2c}) in comparison with that of the crystalline phase¹⁴. The resonance line of the methylene carbon in the noncrystalline phase

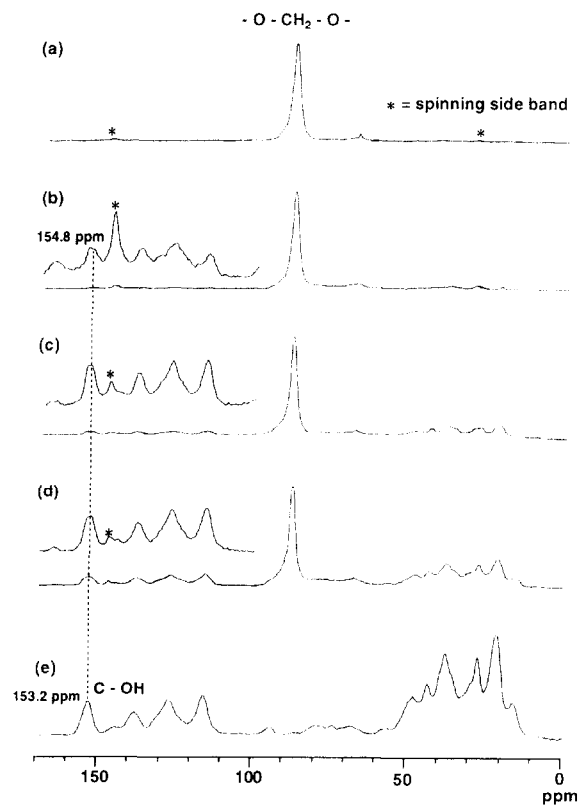


Figure 6 CP/MAS ^{13}C n.m.r. spectra measured at room temperature for different samples: (a) POM; (b) POM/TPh = 9/1; (c) POM/TPh = 7/3; (d) POM/TPh = 5/5; (e) TPh

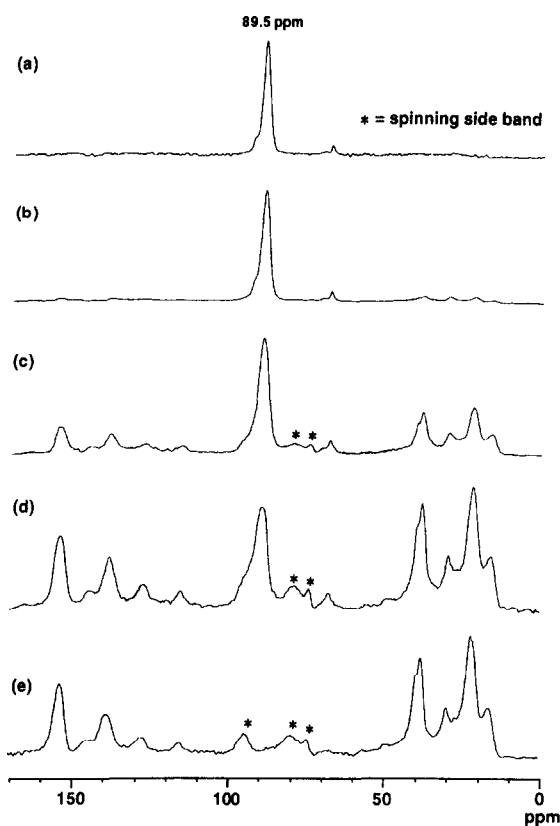


Figure 7 Solid-state ^{13}C n.m.r. spectra measured by ^{13}C spin-echo pulse sequence shown in *Figure 2a*: (a) POM; (b) POM/TPh = 9/1; (c) POM/TPh = 7/3; (d) POM/TPh = 5/5; (e) TPh

is observed at 89.5 ppm and broadened with increasing content of TPh possibly due to the intermolecular interaction with TPh.

On the other hand, ^{13}C n.m.r. spectra measured by the CPT1 pulse sequence emphasize the methylene carbon resonance assigned to the crystalline phase in POM because of its longer ^{13}C spin-lattice relaxation time ($T_{1\text{C}}$)¹⁵. The resonance line of the crystalline phase in POM is observed at 88.2 ppm, and this line is neither shifted nor broadened even after mixing with TPh. From these results, the mixing in this system is concluded to occur preferentially in the noncrystalline phase of POM.

One of possible causes for the line-broadening for the methylene carbon in the noncrystalline phase may be the intermolecular hydrogen-bonding interaction between POM and TPh, which was confirmed by FTi.r. experiments as described above. Another cause of the broadening will be the onset of the molecular motion in the order of 10^4 – 10^5 Hz. When the methylene carbon is subjected to such a molecular motion, ^1H dipolar decoupling efficiency must be lowered resulting in the broadening of the resonance line. Moreover, the signal/noise ratio of CP/MAS spectra should be appreciably decreased as a result of the decrease in $T_{1\rho\text{H}}$, which is also sensitive to the molecular motion in the order of 10^4 – 10^5 Hz. However, it has been found that there is no significant decrease in the signal/noise ratio or in $T_{1\rho\text{H}}$ in this blend system. Therefore, the intermolecular interaction must be closely associated with the line broadening for the methylene carbon of POM.

^1H spin-diffusion experiments

^1H spin-diffusion phenomenon is widely used for a quantitative evaluation of the miscibility of polymer blend systems. When strong dipolar coupling exists between protons belonging to two different polymers as a result of their intimate mixing, efficient spin-exchange is promoted and the protons show an identical spin relaxation time. In contrast, protons far apart or in different environments relax independently of one another or significantly depending on the size of the domains composed of the respective polymers. Thus it is possible to evaluate homogeneity or inhomogeneity of mixing in a polymer blend system by means of the spin relaxation times of protons belonging to two different polymers.

A level of homogeneity of polymer blends is usually estimated in terms of $T_{1\text{H}}$ and $T_{1\rho\text{H}}$ on different scales^{13,16–24}. When the $T_{1\text{H}}$ values are identical for two polymers, this blend system may be homogeneous on a scale of 20–30 nm. In contrast, the identical $T_{1\rho\text{H}}$ values for both polymers suggest their homogeneous mixing on a scale of 2–3 nm. First we have measured $T_{1\text{H}}$ and $T_{1\rho\text{H}}$ values of POM and TPh at room temperature by the pulse sequences conventionally used, which are summarized in *Table 1*. Unfortunately, $T_{1\text{H}}$ and $T_{1\rho\text{H}}$ values for POM and TPh are so close to each other in the pure state that these values are not suitable in evaluating the miscibility of POM/TPh blends.

As an alternative method for evaluating the level of mixing, we have adopted the method combined with the Goldman–Shen pulse sequence⁵ and CP/MAS ^{13}C n.m.r. technique. This method makes it possible to directly observe the ^1H spin-diffusion from one component polymer to another in a polymer blend system. As shown in *Figure 2b*, after the ^1H overall transverse magnetization is created by the first ^1H 90° pulse, a component with a shorter $T_{2\text{H}}$ is selectively allowed to relax to zero during a period of t_1 . The remaining ^1H magnetization with a longer $T_{2\text{H}}$ is set parallel to the static magnetic field by the second ^1H 90° pulse. During a mixing time τ , the ^1H spins then diffuse from the longer $T_{2\text{H}}$ component to the shorter component through the ^1H – ^1H dipolar interaction. The resulting ^1H magnetization is transferred to ^{13}C spins by the cross-polarization technique. Thus the ^1H spin-diffusion process is able to be directly examined as a function of the mixing time τ .

Figure 8 shows CP/MAS ^{13}C n.m.r. spectra for the POM/TPh (5/5) blend measured by the pulse sequence shown in *Figure 2b*. Since the $T_{2\text{H}}$ for the crystalline component of POM in this blend system is shorter than

Table 1 $T_{1\text{H}}$ and $T_{1\rho\text{H}}$ values for POM and TPh measured at room temperature

Resonance line (ppm)	$T_{1\text{H}}$ (s)	$T_{1\rho\text{H}}$ (ms)
POM		
88.5	1.0	24
TPh		
21.6	1.0	20
27.6	1.0	20
38.0	1.1	19
43.6	1.0	19
153.2	1.4	19

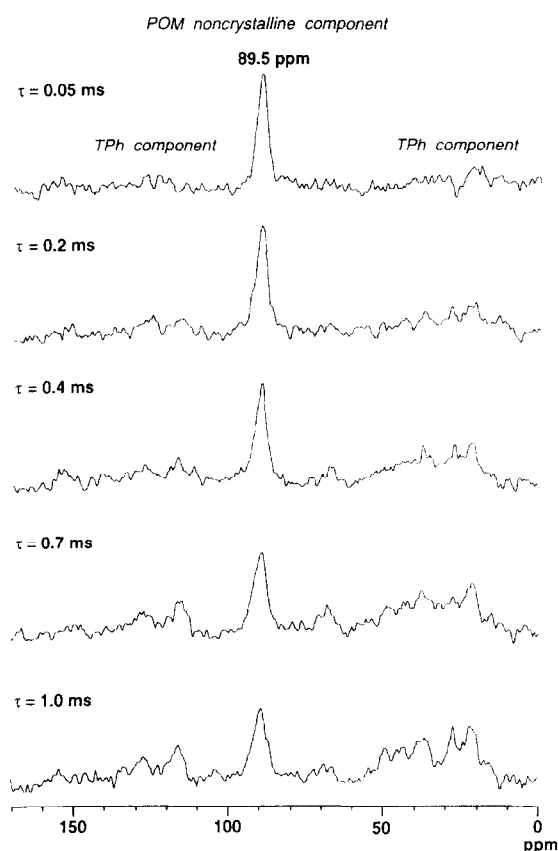


Figure 8 Solid-state ^{13}C n.m.r. spectra for POM/TPh (5/5) blend measured by the pulse sequence shown in Figure 2b at mixing times τ of 0.05 ms to 1.0 ms

Table 2 T_{2H} and t_c values for POM/TPh (5/5) blend estimated by high-resolution solid-state ^{13}C n.m.r. experiments

Resonance line (ppm)	T_{2H} (μs)	t_c^a (ms)
POM (noncrystalline component) 89.5	35.5	1.0
POM (crystalline component) 88.2	7.9	33.6
TPh 21.5	4.4	
27.6	4.1	
38.0	4.2	
43.5	4.1	1.0
153.5	4.5	

^a Pseudoequilibrium values estimated in Figure 10

8 μs , as shown in Table 2, the delay time t_1 was set to 40 μs in this case.

As shown in Figure 8, the resonance line assignable to the noncrystalline component of POM is selectively observed at 89.5 ppm for $\tau = 0.05$ ms. With increasing mixing time τ , the intensity of the noncrystalline line is evidently decreased, while the resonance line assigned to TPh is increased in intensity. As τ further increases, the resonance line at 88.2 ppm assigned to the crystalline part of POM appears and is increased in intensity as shown in Figure 9. These spectral changes are due to the ^1H spin-diffusion from the noncrystalline component of POM to TPh and the crystalline component of POM.

For the estimation of the domain size, an appropriate model should be assumed under consideration of the ^1H

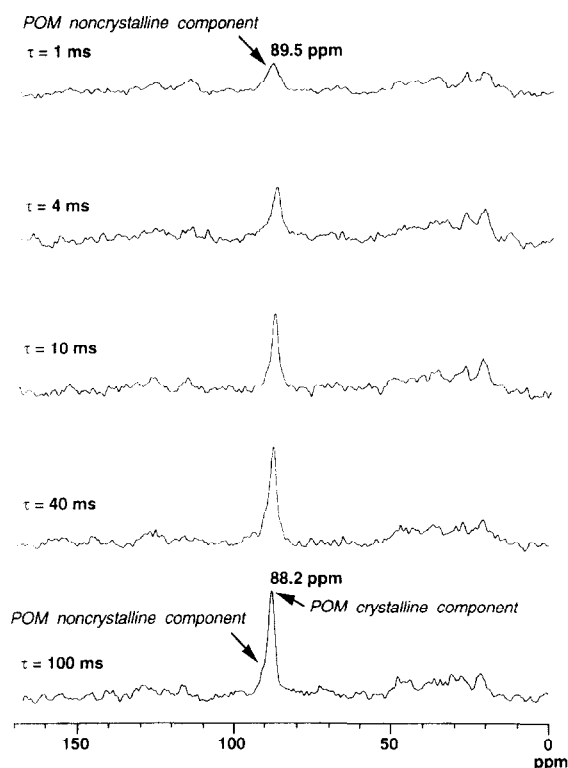


Figure 9 Solid-state ^{13}C n.m.r. spectra for POM/TPh (5/5) blend measured by the pulse sequence shown in Figure 2b at mixing times τ of 1 ms to 100 ms

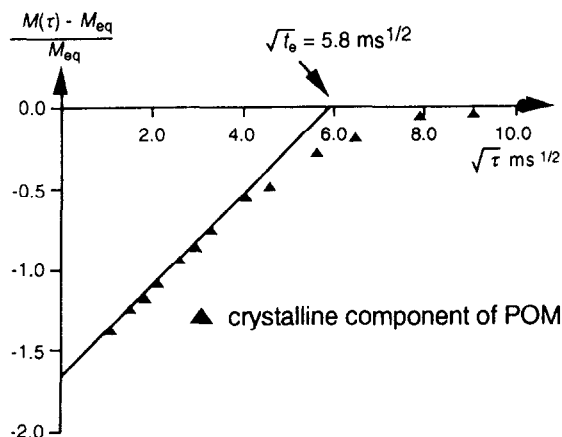
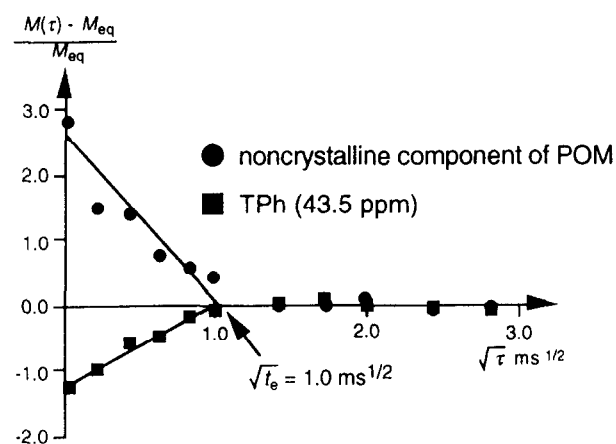


Figure 10 Plots of the reduced ^1H magnetization, $(M(\tau) - M_{eq})/M_{eq}$, vs. the square root of the mixing time τ for the POM/TPh (5/5) blend

spin diffusion process in the micro-phase separated system. The present POM/TPh blend system may be, however, a complicated phase-separated system. Therefore, we have adopted a one-dimensional lamellar structure model as is frequently used in different polymer blend systems^{13,22}. When such a structure model is assumed, the following data treatment is available¹³: $(M(\tau) - M_{\text{eq}})/M_{\text{eq}}$ is plotted against the square root of the mixing time τ as shown in *Figure 10*. Here, $M(\tau)$ is the ^{13}C magnetization at the mixing time τ and M_{eq} is the pseudoequilibrium magnetization at time t_c , where the corresponding magnetization is not further changed through the ^1H spin diffusion. As shown in *Figure 10*, t_c can be determined as a cross-point of the straight line with a slope of 1.0 for the initial plot on the abscissa axis. In this estimation, the resonance line at 43.5 ppm was used as a representative of TPh because of its better signal/noise ratio. The t_c values thus obtained for the noncrystalline component of POM is in good accord with the value for TPh ($t_c = 1.0$ ms), whereas the crystalline component of POM has a longer t_c value ($t_c = 33.6$ ms) as listed in *Table 2*. These results indicate that the ^1H spin-diffusion between TPh and the noncrystalline component of POM attains an equilibrated state quickly within one ms and then proceeds slowly further to the crystalline phase in POM. In other words, the noncrystalline component of POM is more closely mixed with TPh than the crystalline component.

By also assuming the one-dimensional spin-diffusion process, the effective diffusive path length x may be given as mean square form by¹³

$$\langle x^2 \rangle = 4Dt_c/3 \quad (1)$$

where the parameter D is the spin-diffusion coefficient expressed as

$$D = 2r_0^2/T_{2\text{H}} \quad (2)$$

and r_0 is the proton van der Waals radius of 0.117 nm. The $\langle x^2 \rangle$ value is determined to be 1.03 nm² for the noncrystalline phase in the POM/TPh (5/5) blend, using the $T_{2\text{H}}$ value of 35.5 μs and t_c value of 1.0 ms. This indicates that the average size for the domains, which are composed of the noncrystalline POM and TPh in this blend, is of the order of 1 nm.

CONCLUSIONS

TEM observations provided information about the homogeneity on a scale of a μm for the POM/TPh blend system. FTi.r. experiments revealed that the intermolecular hydrogen-bonding interaction exists between POM and TPh in their blend systems. On the other hand, selective high-resolution solid-state ^{13}C n.m.r. measurements, which were based on the spin-echo and CPT1

pulse sequences, were found to be very useful in examining the mixing states in the noncrystalline and crystalline phases separately: TPh was preferentially mixed with POM in the noncrystalline phase probably through the intermolecular hydrogen-bonding interaction, which was confirmed by the ^{13}C spectra of the methylene and phenolic carbons. In contrast, there was no spectroscopic evidence for the association of TPh in the crystalline phase of POM. Separate ^1H spin-diffusion analysis revealed that the phase-separated domain size is of the order of 1 nm in the noncrystalline phase in this blend system.

ACKNOWLEDGEMENT

We thank Ms K. Matsuda for her assistance in FTi.r. measurements.

REFERENCES

- 1 Wang, X., Saito, H. and Inoue, T. *Kobunshi Ronbunshu* 1991, **48**, 443
- 2 Machado, J. M. and French, R. N. *Soc. Plast., Eng. Ann. Tech. Conf.* 1991, **49**, 1586
- 3 French, R. N., Machado, J. M. and Lin-Vien, D. *Polymer* 1992, **33**, 755
- 4 Torchia, D. A. *J. Magn. Reson.* 1978, **30**, 613
- 5 Goldman, M. and Shen, L. *Phys. Rev.* 1966, **144**, 321
- 6 Trent, J. S., Scheinbeim, J. I. and Couchman, P. R. *Macromolecules* 1983, **16**, 589
- 7 Takamatsu, S., Kobayashi, T., Komoto, T., Sugiura, M. and Ohara, K. *Polymer* 1994, **35**, 3598
- 8 Coleman, M. M. and Painter, P. C. *Appl. Spectrosc. Rev.* 1984, **20**, 255
- 9 Zamboni, V. and Zerbi, G. *J. Polym. Sci.* 1964, **C7**, 153
- 10 Oleinik, E. F. and Enikolopyan, N. S. *J. Polym. Sci.* 1968, **C16**, 3677
- 11 Terlemezyan, L. and Mihailov, M. *Eur. Polym. J.* 1981, **17**, 1115
- 12 Shimomura, M., Iguchi, M. and Kobayashi, M. *Polymer* 1988, **29**, 351
- 13 VanderHart, D. L. *Makromol. Chem., Macromol. Symp.* 1990, **34**, 125
- 14 Komoroski, R. A. (Ed.) 'High Resolution NMR Spectroscopy of Synthetic Polymers in Bulk', VCH Publishers, Florida, 1986, Chapter 5
- 15 Veeman, W. S., Menger, E. M., Ritchey, W. and de Boer, E. *Macromolecules* 1979, **12**, 924
- 16 McBrierty, V. J., Douglass, D. C. and Kwei, T. K. *Macromolecules* 1978, **11**, 1265
- 17 Douwel, C. H. K., Maas, W. E. J. R., Veeman, W. S., Buning, G. H. W. and Vankan, J. M. *J. Macromolecules* 1990, **23**, 406
- 18 Zhang, X., Takegoshi, K. and Hikichi, K. *Polym. J.* 1991, **23**, 87
- 19 Zhang, X., Takegoshi, K. and Hikichi, K. *Macromolecules* 1991, **24**, 5756
- 20 Masson, J. F. and Manley, R. S. *J. Macromolecules* 1991, **24**, 5914
- 21 Masson, J. F. and Manley, R. S. *J. Macromolecules* 1992, **25**, 589
- 22 Zhang, X., Takegoshi, K. and Hikichi, K. *Macromolecules* 1992, **25**, 2336
- 23 Jong, L., Pearce, E. M. and Kwei, T. K. *Polymer* 1993, **34**, 48
- 24 Schmidt, P., Straka, J., Dybal, J., Schneider, B., Doskocilova, D. and Puffr, R. *Polymer* 1995, **36**, 4011